Polymer(Korea), Vol. 43, No. 2, pp. 169-180 (2019)
https://doi.org/10.7317/pk.2019.43.2.169

ISSN 0379-153X(Print)
ISSN 2234-8077(Online)

수분산 폴리우레탄 코팅의 미세상분리와 물성에 Isosorbide가 미치는 영향

Jun Hu, Can Tao, Aining Yuan, Junjie Bao, Qin Cheng, Gewen Xu, and Yiping Huang†

School of Chemistry and Chemical Engineering, Anhui University

(2018년 7월 6일 접수, 2018년 11월 8일 수정, 2018년 12월 28일 채택)

Effects of Isosorbide on the Microphase Separation and Properties of Waterborne Polyurethane Coatings

Jun Hu, Can Tao, Aining Yuan, Junjie Bao, Qin Cheng, Gewen Xu, and Yiping Huang†

School of Chemistry and Chemical Engineering, Anhui University, Key Labortory of Environment-friendly Polymer Materials of Anhui Province, Hefei 230601, People's Republic of China

(Received July 6, 2018; Revised November 8, 2018; Accepted December 28, 2018)

Abstract: Series of waterborne polyurethanes (WPUs) containing poly(tetra methylene glycol) (PTMG), 4,4-dicyclohexylmethane diisocyanate (HMDI), 2,2-dimethylolpropionic acid (DMPA), 2,2,4-trimethyl-1,3-pentanediol (TMPD), isosorbide (ISO) and ethylenediamine (EDA) were synthesized. The effects of ISO on the structure and properties of WPUs were studied by gel permeation chromatography (GPC), Fourier-transform infrared spectroscopy (FTIR), differential scanning calorimetry (DSC), dynamic mechanical analyzer (DMTA), X-ray diffraction (XRD), thermogravimetry (TG), mechanical test, chemical resistance and hardness test. The deconvolution analysis of FTIR of WPUs revealed that the hydrogen bond interaction in the WPUs increased with the increase of ISO content. Furthermore, the degree of microphase separation was increased with the increase of hydrogen bond interaction, which was confirmed by DSC, XRD and DMTA test. The results demonstrated that the addition of ISO can increase the hydrogen bond interaction between the hard and hard segments in WPUs, which improved the mechanical properties of the WPU films. The highest tensile strength was obtained of 59.67 MPa when the content of isosorbide was 10.35 wt%. Moreover, the ISO was helpful to improve the chemical resistance and hardness of the coatings by the comprehensive performance analysis.

Keywords: isosorbide, micro-phase separation, waterborne polyurethane, mechanical properties.

Introduction

Isosorbide (ISO) is a green, nontoxicity and renewable biomaterial which has been widely used in synthesis of polyesters, polyethers, polyamides and polycarbonates. Isosorbide can offer high rigidity and improve thermal stability to the synthesized ISO-based polymers.[1-3] Recently, biomass-based polyurethanes from ISO have attracted increasing attention because ISO possesses two hydroxyl groups which makes it very suitable for polyurethane synthesis as chain extender.[4-6] With the addition of ISO, the glass transition temperature of hard segments of synthesized ISO-based polyurethanes was significant increased which has been confirmed by Marín *et al*. and Calvo-Correas *et al*..[7,8] Moreover, the ISO can also increase the tensile strength of ISO-based polyurethanes.[9] The changes in the properties of polyurethanes are associated to the effects of ISO on the morphology. Javni *et al*. found that the hard domain size and the mean separation distance of thermoplastic polyurethanes were decreased with the increasing of ISO content.[10] Research results from Oprea *et al*.[4] and Blache *et al*.[5] revealed that ISO decreased the phase separation of polyurethane. Due to the growing consciousness on environmental concerns regarding hazardous air pollutants, waterborne polyurethanes (WPUs) have attracted increasing attention.[11,12] However, compared to solvent polyurethane, a number of flaws like the poor mechanical properties, inferior thermal properties and solvent resistance limited the usage of WPUs especially for coatings.[13-15] Due to the rigid V-shaped bicyclic structure of ISO, the incorporation of ISO into the WPUs backbone could improve its mechanical properties and solvent

†To whom correspondence should be addressed.
yphuang@sina.com.cn, ORCID 0000-0003-2353-5561

resistance. Hence, a few works on ISO-based WPUs have been investigated.[16-18] Xia *et al.*[16] prepared a series of soybean oil-ISO-based WPUs by varying ISO content. When the ISO amount was increased from 0 to 20 wt%, the Young's modulus and the ultimate tensile strength of soybean oil-ISO-based WPUs were increased from 2.3 to 63 MPa and 0.7 to 8.2 MPa, respectively. Li *et al.*[17] found that the high ISO content was in favor of good acetone resistance and moderate impact resistance of WPU coatings which applied on aluminum panels. Some ISO-based WPUs with three chain extenders (EDA, ADH and water) have been prepared but these WPUs were still not available for coatings.[18]

To our best knowledge, ISO-based WPUs with high strength, hardness, solvent resistance and excellent adhesion for coatings are not mentioned in previous literatures. Furthermore, the effects of ISO on the hydrogen bond interactions and microphase separation of ISO-based WPUs are not investigated clearly. In this work, the effects of ISO content on the properties of ISO-based WPUs were investigated. Serious of WPUs with different ratio of ISO and 2,2,4-trimethyl-1,3-pentanediol (TMPD) were synthesised. The hydrogen bond interactions were studied by Fourier-transform infrared spectroscopy (FTIR). The microphase separation of ISO-based WPUs was investigated by DSC, XRD and DMA tests. The ISO-based WPUs with good mechanical properties, thermal stability, hardness, chemical resistance and adhesion are much suitable for the usage of coatings.

Experimental

Materials. Poly(tetra methylene glycol) (PTMG1000, PTMG2000, Industrial grade) was purchased from Mitsubishi in Japan; 4,4-dicyclohexylmethane diisocyanate (HMDI, Industrial grade) was purchased from Degussa AG; 2,2-dimethylolpropionic acid (DMPA, Industrial grade) was obtained from Perstop; Isosorbide (ISO, analytical purity), 2,2,4-trimethyl-1,3-pentanediol (TMPD, analytical purity), triethylamine (TEA, analytical purity) were supplied by Sa en Chemical Technology Co., Ltd.. Shanghai in China. Ethylenediamine (EDA, analytical purity) was obtained from Tai cang Shanghai Test Reagent Co., Ltd.. Acetone (AC, analytical purity) was supplied by Shanghai Shen Bo Chemical Co., Ltd.; stannous octoate (T9, analytical purity) and dibutyltin dilaurate (T12, analytical purity) was supplied by Beijing Chemical Factory.

Synthesis of Waterborne Polyurethane Dispersions. The mass ratios of the reagents of WPU are listed in Table 1. The synthetic route of WPU is shown in Scheme 1. First, PTMG1000, PTMG2000, ISO and TMPD which dried in a vacuum at about 100 °C for 1 h and poured into a 250 mL four-necked flask equipped with a reflux condenser, a thermometer and a mechanical stirrer. Then the HMDI was added into the mixture. The mixture was reacted at 90±2 °C under the protection of N_2. After reacting about 2.5 h, the DMPA dissolved in AC was added into the flask and reacted at 80±2 °C for 1 h. Subsequently, the T9 and T12 were added into the flask and reacted at 70±2 °C until the content of –NCO reached the theoretical value. The acetone was slowly added to adjust the viscosity of the prepolymer. Then, the TEA used as a neutralizing agent and the distilled water were added into the flask and stirred with the rate of 1300 r/min for 2 min. Afterwards, the EDA was added into the mixture when the temperature was maintained at about 40 °C. Finally, the WPU dispersion was obtained after the acetone was removed under vacuum.

Preparation of WPU Films. The emulsion was poured into a Teflon plate and dried naturally for 3 days. After a large amount of water was volatilized, meanwhile, the surface of the film was dried basically, and then the film was taken out and placed in a vacuum oven. The film was dried at 50 °C under vacuum until its mass no longer changed for further testing.

Characterizations. The Particle Size and Distributions: The average particle size and distributions of WPU emulsion

Table 1. Mass Ratios of the Reagents of WPU

Samples	HMDI (g)	PTMG1000 (g)	PTMG2000 (g)	DMPA (g)	EDA (g)	ISO (g)	TMPD (g)	W_{ISO} (%)
WPU1	42.50	24.00	6.00	3.80	1.89	8.81	0.00	10.35
WPU2	42.50	24.00	6.00	3.80	1.89	6.81	2.00	8.00
WPU3	42.50	24.00	6.00	3.80	1.89	5.11	3.70	6.00
WPU4	42.50	24.00	6.00	3.80	1.89	3.40	5.41	4.00
WPU5	42.50	24.00	6.00	3.80	1.89	1.70	7.11	2.00
WPU6	42.50	24.00	6.00	3.80	1.89	0.00	8.81	0.00

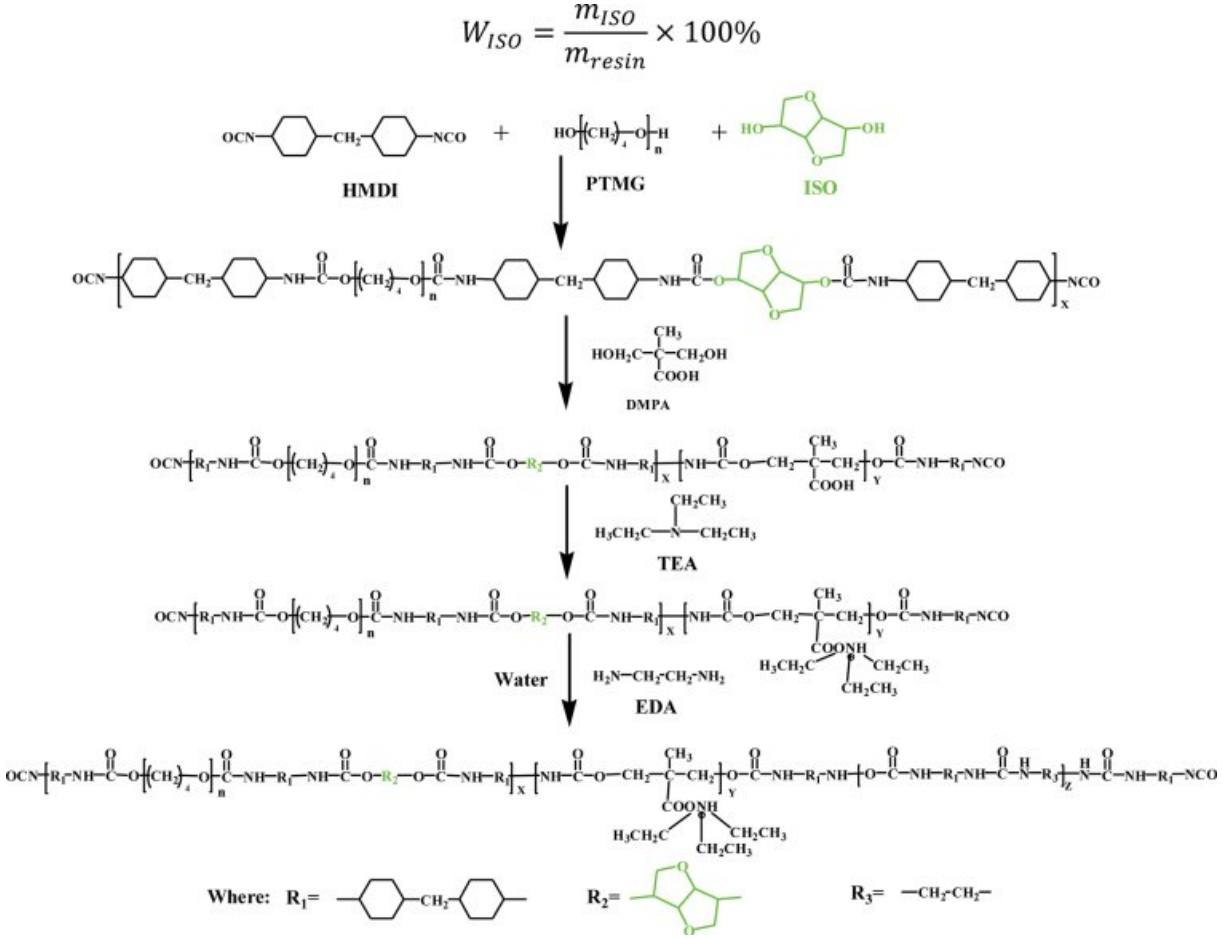

Scheme 1. Synthetic route of WPU.

were tested in Malvern ZetaSizer Nano-ZS90 (Malvern, UK) at 25 ºC, and the emulsion concentration was diluted to 3‰ by deionized water. The laser scattering angle is set at 90º.

Gel Permeation Chromatography (GPC): The number-average molecular weights of WPU were determined by GPC (Hewlett-Packard 1100) with polystyrene as the calibration standard. The solvent was THF, the flow rate of mobile phase was 1.00 mL·min^{-1}, the temperature was 25 ºC, injection volume was 20.00 μL, sample content was 0.3%.

Fourier Transform Infrared Spectroscopy (FTIR): The ATR-IR spectra of WPU films were recorded on Nexus-870 Infrared spectrometer (ATR) (Nicolet, USA) with the wavenumber range of 600-4000 cm^{-1}, a resolution of 2 cm^{-1}, and a scan number of 32.

Differential Scanning Calorimetry (DSC): WPU films were thermally analyzed by differential scanning calorimetry (DSC, TA Instruments, USA) under a nitrogen atmosphere, and the sample mass was 7 to 10 mg. The samples were heated to 200 ºC for 3 min to eliminate thermal history with the heating rate of 20 ºC/min, then cooled to -80 ºC/min to keep 5 min with the rate of 20 ºC/min. Finally, the samples were heated to 200 ºC with the heating rate of 20 ºC/min. The result was recorded from the cooling scan to the second heating scan.

Dynamic Mechanical Thermal Analysis (DMTA): The viscoelastic properties of WPU films were measured by dynamic mechanical thermal analyzer (DMTA, TA Instruments, and USA). The thickness of the films was controlled below 0.5 mm, the dimension of the sample was 25 mm× 4 mm, and the test temperature was -80~200 ºC with a heating rate of 5 ºC/min, the frequency was 1 Hz.

X-ray Diffraction (XRD): The crystallinity of WPU films was characterized using a Japanese XD-3 X-ray diffractometer. The dimension of the sample was 1 cm×1 cm×0.4 cm. The scanning rate of 5 (º)/min, a sampling width of 0.02º, and an angle scanning range of 5º to 80º.

Mechanical Properties: Tensile properties were measured

on XLW-500 intelligent electronic tensile testing machine (Shenzhen San si Materials Testing Co., Ltd.).The dimension of WPU film was 25 cm×4 cm, the tensile rate of 200 mm/min, the test temperature was room temperature, and each sample test three times to take the average.

Thermal Gravimetric Analysis (TG): The thermal degradation and structure of WPU films were studied in Pyris-1 thermogravimetric analyzer (netzsch, Germany) under nitrogen atmosphere. The temperature range was from room temperature to 600 ºC, the heating rate was 20 ºC/min, and the sample quality was 7~10 mg.

The Contact Angle: The contact angle of WPU films were measured by contact angle measuring instrument (DSA10-MK2, KRUSS, Germany). The test temperature was 25 ºC. Each film was tested at three different points and averaged.

The Chemical Resistance: The test results of the chemical resistance were expressed in liquid absorption. The dimension of WPU films was 4 cm×4 cm, the sample initial mass was m_0, and the samples were soaked in water, acetone, ethanol (99.5%) and DMF (*N*,*N*-dimethylformamide) for 24 h, then take out and dry the surface, the sample mass was m_1. WPU films in the liquid absorption rate according to the following formul:

$$W\% = \left[\frac{(m_1 - m_0)}{m_0}\right] \times 100\% \quad (1)$$

The Pencil Hardness: The pencil hardness of WPU films was measured according to GB/T 6739-1996. Samples were produced according to GB/T 3186-2006.

The Adhesion: The adhesion of WPU films was measured according to GBT9286-1998. The paint film on the tinplate was scratched according to GB/T 1727-92 and then cut 100 small squares of parallel and equal spacing on the coating by using the cross-cutting blade, brushed off the chips with a soft brush. The adhesive coating was peeled off the 3M tape to observe the peeling state of the coating after the coating was pulled apart. The test temperature was 23±2 ºC and the relative humidity was 50±5%.

Results and Discussion

Structure Analysis. Figure 1 shows the FTIR spectra of WPU films. The disappearance of bands at 2270 cm^{-1} with the appearance of N-H stretching around at 3500~3100 cm^{-1} and C=O stretching at 1750~1595 cm^{-1} in all samples indicated that the polymerization reaction was completed. The C-H stretching of the methyl groups and methine groups is found at 2984~2801 cm^{-1}. The C=O stretching is loacted at 1772~1595 cm^{-1}. The C-N stretching of carbamate appears at 1530 cm^{-1} and the C-O-C stretching of ether oxygen is found at 1170~1054 cm^{-1}.

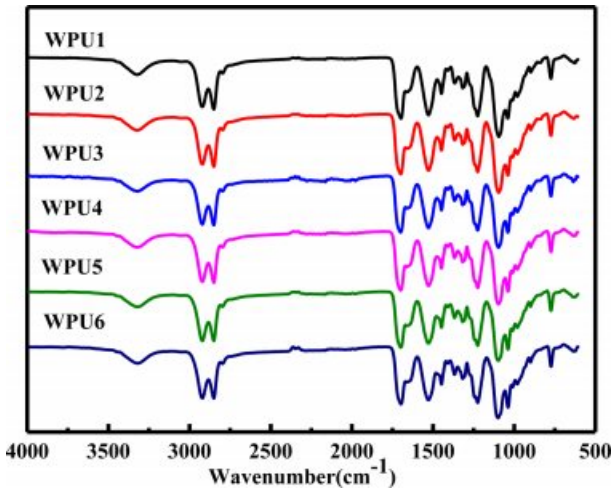

Figure 1. FTIR spectra of WPU films.

It is well known that the C=O and N-H bands were two typical bands for the study of hydrogen bond interactions in polyurethanes.[19] Hydrogen bonds were formed by the N-H groups acting as proton donors and oxygen in the carbonyl of the hard segment and in etheroxy of the soft segments as proton acceptors.[20] As shown in Figure 1, the position of N-H stretching vibration peak was moved to the low wavenumbers. It indicates that hydrogen bond interactions have changes when ISO was introduced to the system. The effects of ISO on the hydrogen bond formation were investigated in the N-H stretching region, the carbonyl stretching region, and the etheroxy stretching region based on the FTIR spectra of WPUs.

The peak around at 3500~3100 cm^{-1} could be separated into two peaks by deconvolution analysis. The results are shown in Figure 2(a) to (f) and Table 2. The peak around at 3520~3480 cm^{-1} is ascribed to the free N-H stretching vibration peak area, and the peak around at 3400~3100 cm^{-1} is for the hydrogen bonded N-H stretching vibration peak.[21,22] With the increased of W_{ISO}, the location of the peak and the value of N-H in the hydrogen bond interaction slightly increased. Compared with WPU6, the hydrogenated N-H stretching vibration peak area increased significantly from WPU1 to WPU5. This result might be attributed to the structure of ISO having C=O bands so that the free N-H band was easier hydrogenated in the system. Therefore, the hydrogen bond interaction between

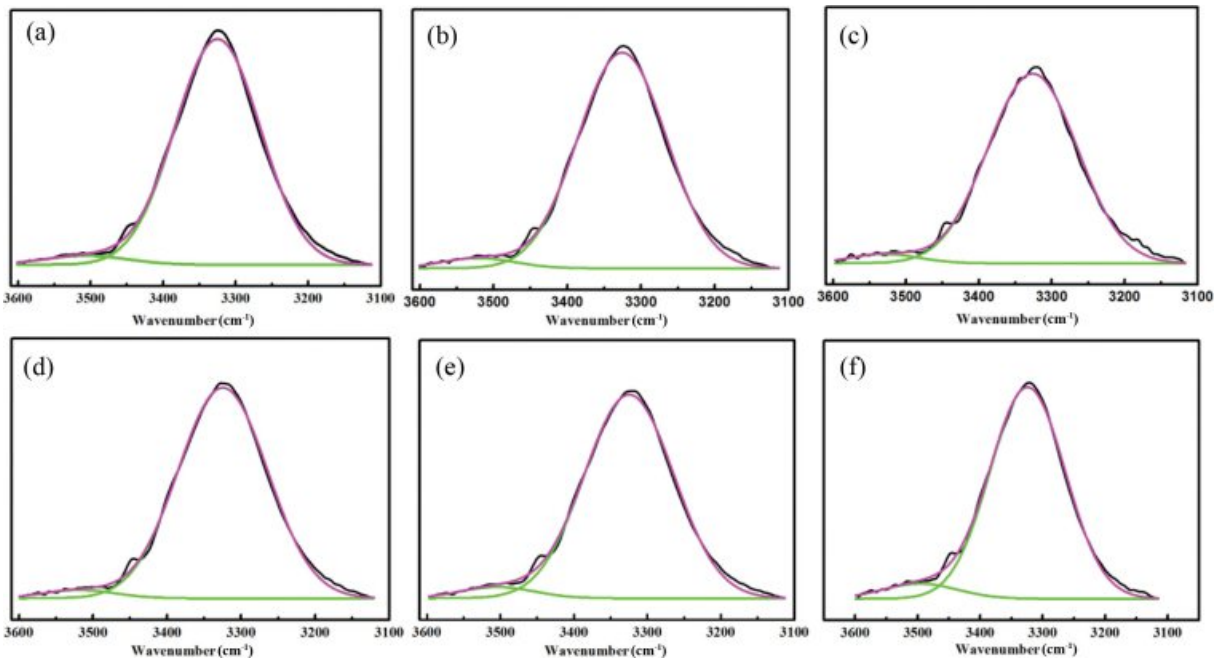

Figure 2. Deconvoluted FTIR spectrum of sample WPUs (a-f): Amino stretching region.

Table 2. Relative Areas under the Various FTIR Bands in Amino Stretching Region

	Peak position (cm^{-1})		Peak area ratio (%)	
Samples	Free N-H	Bonded N-H	Free N-H	Bonded N-H
WPU 1	3506	3324	3.65	96.35
WPU 2	3520	3325	3.53	96.47
WPU 3	3528	3326	3.27	96.73
WPU 4	3518	3324	2.89	97.10
WPU 5	3504	3324	4.23	95.77
WPU 6	3496	3324	6.33	93.67

hard and hard segments is strengthened. It was necessary to further conduct the deconvolution analysis of the carbonyl group and the etheroxy group to research the effect of ISO on hydrogen bond interaction of WPUs.

Figure 3(a) to (f) and Table 3 show the deconvolution of the C = O stretching vibration peak of WPUs. The peak around at 1740~1720 cm^{-1} is ascribed to the free C=O stretching vibration peak area, the peaks around at 1720~1690 cm^{-1} and 1660~1640 cm^{-1} are for the absorption peak corresponding to disorder and ordered hydrogenated C=O regions.[22,23] It can be seen from Table 3 that the value of the free region of the C=O stretching vibration and the value of the ordered region of the C=O stretching vibration was decreased with decreasing the content of ISO. The disordered region of C=O stretching vibration increased with the content of ISO decrease. It shows the degree of hydrogen bond interaction of C=O stretching vibration of WPU decreased when the content of ISO increased. The reason might be that the etheroxy group structure of ISO and NH bands is easier hydrogenated compared with carbonyl group. However, the value of N-H in the hydrogen bond interactions increased and the value of C=O in the hydrogen bond interactions decreased. So etheroxy groups were hydrogenated with amino. Deconvolution analysis of ether oxygen was prerequisite.

Figure 4(a) to (f) and Table 4 show the deconvolution of the C-O-C stretching vibration peak of WPUs. The peaks around at 1172~1100 cm^{-1} are for the free C-O-C stretching vibration peak area. The peaks around at 1100~1080 cm^{-1} are for hydrogenated C-O-C stretching vibration peak area.[22,24] As shown in Table 4, the value of the free region of the C-O-C stretching vibration decreased, and the value of the hydrogen bond region of the C-O-C stretching vibration increased when the content of ISO increased. It is consistent with the carbonyl deconvolution analysis.

From the above analysis, the ISO could increase the degree of hydrogen bond interaction in the WPUs. Because the etheroxy group structure in ISO, which mainly destroyed the hydrogen bond interaction of N-H and C=O bonds. Meanwhile, N-H and the ISO of C-O-C bond hydrogen bond interaction increased, and ISO belongs to the hard segment in the

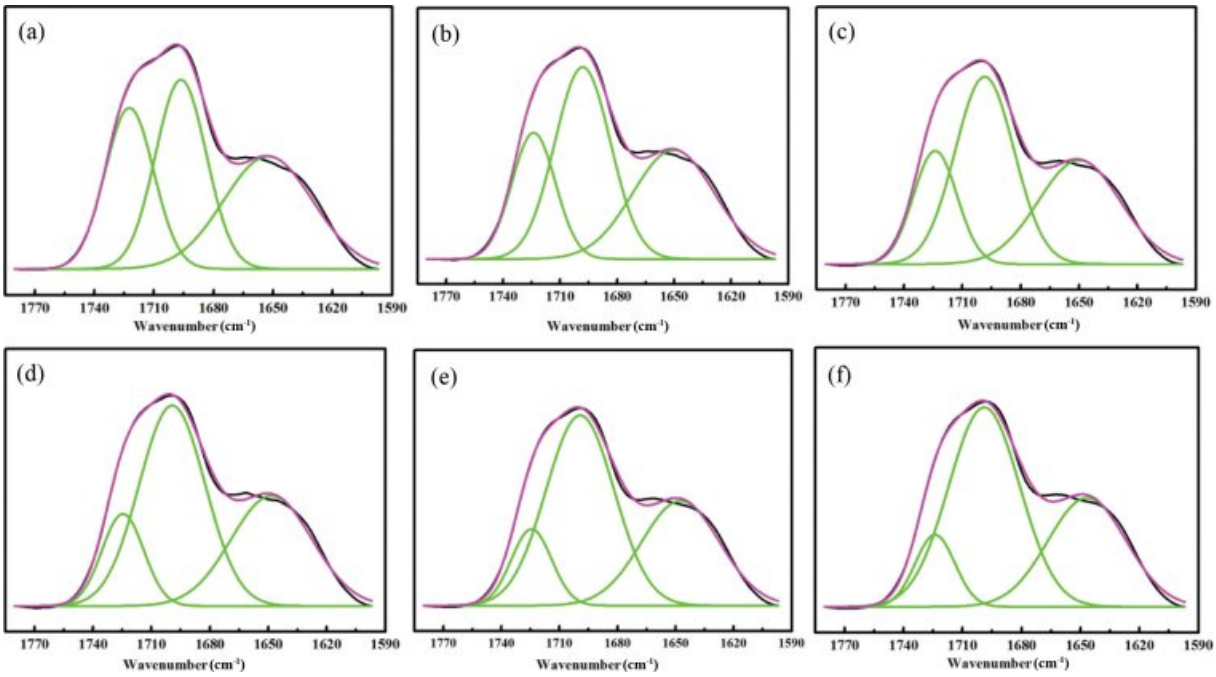

Figure 3. Deconvoluted FTIR spectrum of sample WPUs (a-f): carbonyl stretching region.

Table 3. Relative Areas under the Various FTIR Bands in Carbonyl Stretching Region

	Peak area (cm^{-1})			Peak area ratio (%)		
Samples	Free C=O	Disorder C=O	Order C=O	Free C=O	Disorder C=O	Order C=O
WPU 1	1722	1696	1652	28.53	35.06	36.41
WPU 2	1723	1698	1650	21.90	42.80	35.29
WPU 3	1724	1698	1649	20.17	45.18	34.64
WPU 4	1724	1699	1648	14.82	51.04	34.13
WPU 5	1724	1699	1647	12.70	53.67	33.63
WPU 6	1723	1699	1646	11.19	55.55	33.26

WPUs. So the hydrogen bond interaction between hard and hard segments is strengthened so that microphase separation of soft and hard segments is increased.

Phase Structure Analysis. The DSC curves of WPUs are shown in Figure 5. The corresponding glass transition temperature (T_g) data are listed in Table 5. The dates show that the soft segment ($T_{g,s}$) and the hard segment T_g ($T_{g,h}$) was increased with the content of ISO increased. But the $T_{g,h}$ was significant increased, and ΔT_g (difference between $T_{g,h}$ and $T_{g,s}$) was also increased, which indicated the degree of micro-phase separation between the soft segment and the hard segment increased. This result might be attributed to two reasons. Firstly, the rigidity ISO limited the movement of the soft segment so that the value of T_g gradually increased. Secondly, with the content of ISO increased, the degree of hydrogen bond increased between the hard segment and the hard segment.[25] We can found that the result was consistent with the infrared analysis.

DSC had roughly demonstrated the degree of changes of micro-phase separation in the WPUs. However, DMTA test could more accurately prove the accuracy of DSC and FTIR results. Figure 6 shows the dynamic mechanical behavior of WPU films. As seen from Figure 6(a), the storage modulus of the samples shows almost no change under 45 ºC, indicating that the systems had a higher storage modulus under 45 ºC. With the increase of temperature, the storage modulus begins to slowly decreased. Then the storage modulus of samples decreased obviously about 45 ºC, which corresponds to the pri-

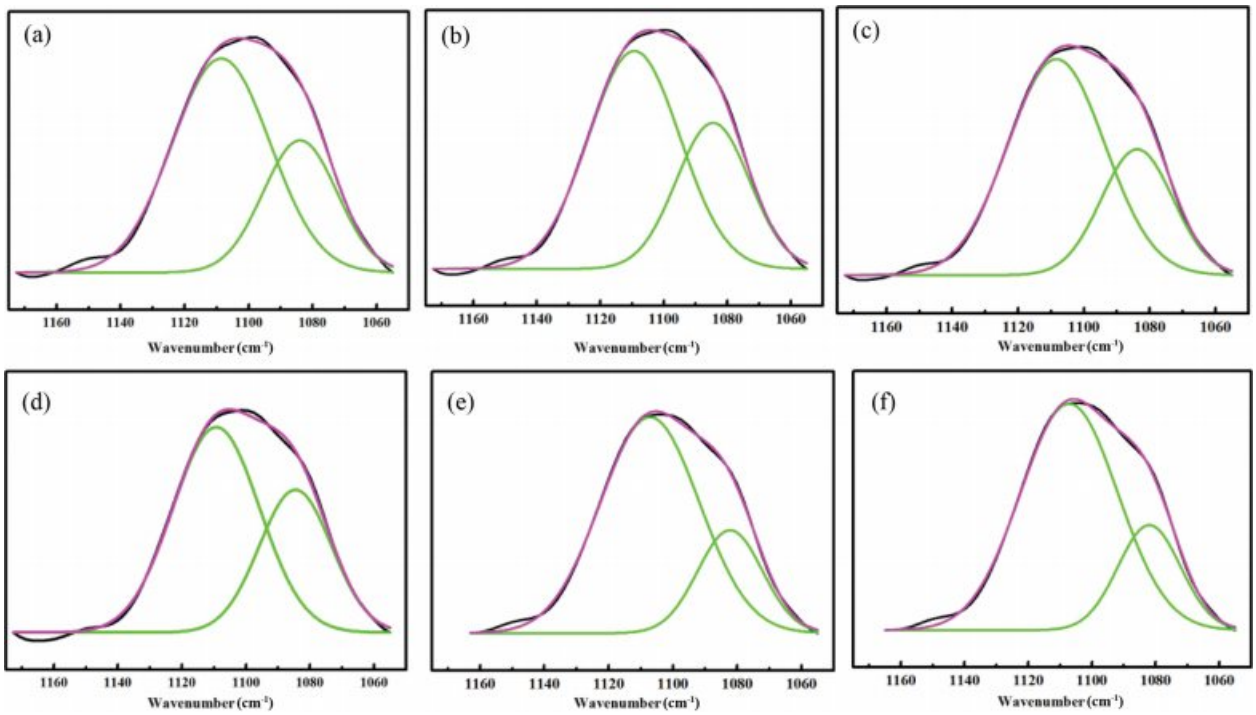

Figure 4. Deconvoluted FTIR spectrum of sample WPUs (a-f): etheroxy stretching region.

Table 4. Relative Areas under the Various FTIR Bands in Etheroxy Stretching Region

	Peak position (cm^{-1})		Peak area ratio (%)	
Samples	Free C-O-C	Hydrogen bonded C-O-C	Free C-O-C	Hydrogen bonded C-O-C
WPU 1	1108	1084	68.21	31.79
WPU 2	1108	1083	69.13	30.86
WPU 3	1108	1083	69.91	30.09
WPU 4	1107	1082	72.35	27.65
WPU 5	1107	1082	76.28	23.72
WPU 6	1107	1082	77.07	22.93

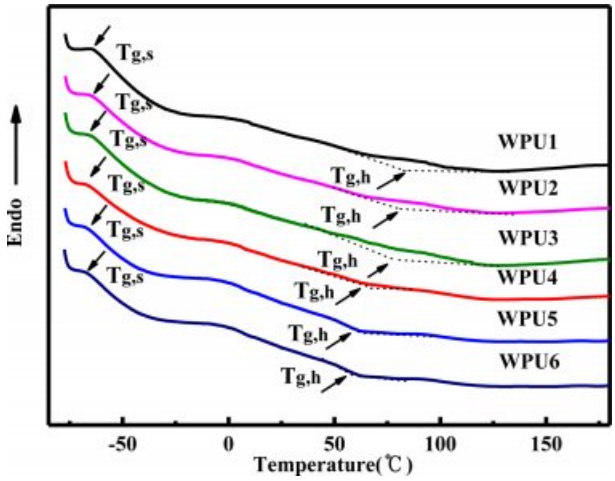

Figure 5. DSC curves of WPU films.

Table 5. Thermal Properties of the WPU Films (unit: °C)

Samples	$T_{g,s}$	$T_{g,h}$	ΔT_g	$T_{d,urea,max}$ [1]	$T_{d,urethane,max}$ [2]	$T_{d,soft,max}$ [3]
WPU1	-63	82	145	337	392	472
WPU2	-64	80	144	310	380	458
WPU3	-65	77	142	318	376	454
WPU4	-65	65	130	317	375	453
WPU5	-66	62	128	317	372	454
WPU6	-67	60	127	316	373	452

mary relaxation process (α), indicating that samples gradually entered the glass transition state. As the content of ISO increased, the process of transformation became slower. Meanwhile, the corresponding logarithms of storage modulus show the maximum value. It might be attributed to the fact that the hydrogen bond interaction provides a network of crosslinks. Moreover, as the temperature increased, hydrogen bonds gradually dissociated so that physical crosslinks also became weaker. As seen from Figure 6(b), the glass transition tem-

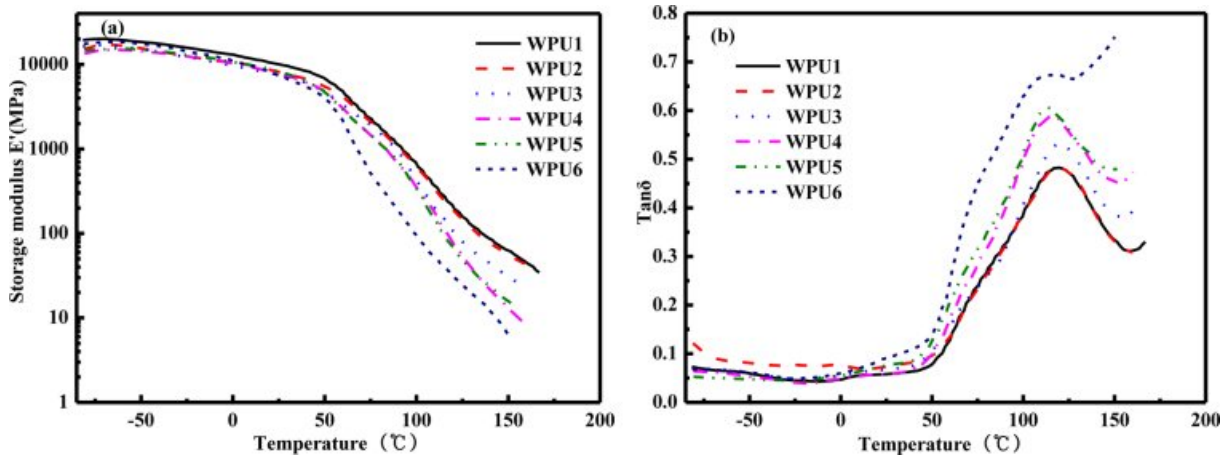

Figure 6. DMTA curves results of WPU films: (a) logarithm of storage modulus (*E'*); (b) tangent of loss angle (tan δ).

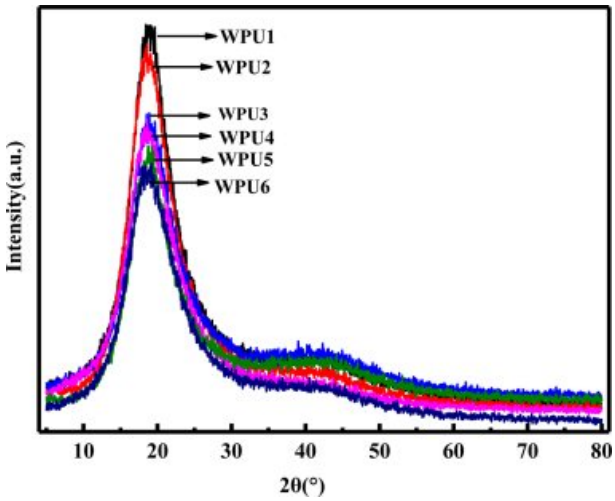

Figure 7. XRD curves of WPU films.

perature of the hard segment ($T_{g,h}$) can be observed for all samples. In summary, these results showed that the WPUs containing ISO increase microphase separation between hard segment and hard segment.[26]

Figure 7 shows the XRD curves of WPU films. It can be seen that the amorphous diffraction peaks are observed near 2θ=20° and 2θ=40°. The dispersion peak of WPUs was related to the hydrogen bond interaction in the ISO-based WPUs segment structure.[27] Compared with WPU6, the diffraction peak intensity of ISO-based WPUs is enhanced, indicating that the ordered hard segment area of ISO-based WPUs increased. The introduction of isosorbide leads to easily hydrogen bonding between the amino groups and the etheroxy groups in the hard segments, which is in favors of the tendency of hard segment regions to an ordered structure. We can see that the result was consistent with the conclusion of infrared analysis.

GPC Analysis. The molecular weight of the WPU was characterized by GPC. The detailed molecular weight (M_n, M_w) and polydispersity index (PDI) of WPUs are summarized in Table 6. It can be seen from the Table 6, the molecular weight of WPU almost unchanged and maintained about 30000. According to the FTIR analysis results, WPU1 and WPU2 contain more isosorbide and involved more hydrogen bonds forming more physical crosslinking network.[28] So WPU1 and WPU2 have better solvent resistance, compared with WPU3-WPU6.

Emulsion Particle Size Analysis. Figure 8 shows the particle size distributions and average particle size of WPU dispersions with different content of ISO. As shown in Figure 8(a), the particle size distribution shows a single peak and the peak firstly became narrow then unchanged when the content of ISO decreased in WPU dispersions. Figure 8(b) shows the

Table 6. Molecular Weight and Polydispersity Index of WPU Films

Samples	WPU1	WPU2	WPU3	WPU4	WPU5	WPU6
M_n	--	--	31891	33373	29205	26996
M_w	--	--	55685	56877	50702	46416
PDI	--	--	1.75	1.70	1.74	1.72

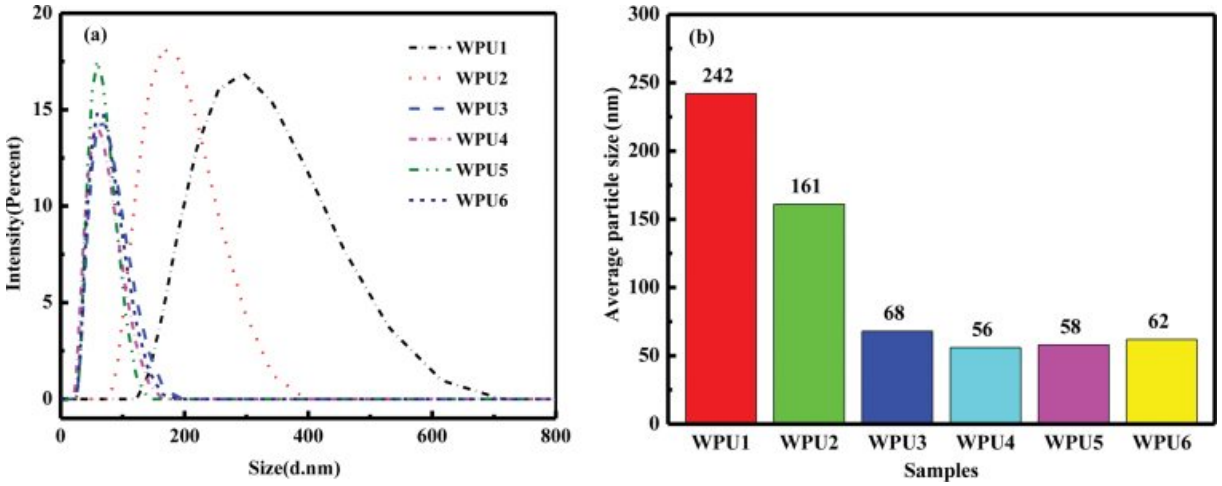

Figure 8. Particle size distribution (a); average particle size (b) of the WPU dispersions.

average particle size firstly became smaller and then unchanged. It might be the result of two reasons. Firstly, ISO is a non-conjugated fused ring structure and large rigidity,[29] thus more difficult to curl in the polyurethane molecular chain which leaded to the change of phase process to slow down. Eventually the emulsion size increases and the particle size distribution broadens.[30] Secondly, the appropriate content of ISO had certain degree of hydrophilicity, which was helpful to emulsification.[31] Hence, the particle size unchanges when the system added suitable content of ISO.

Mechanical Properties. Figure 9 shows the stress-strain curves of WPU films. It can be seen that the tensile strength of WPU films increased when the content of ISO changed. The tensile strength of samples WPU1~WPU6 were 59.67, 47.70, 45.86, 42.87, 42.80, and 38.72 MPa, with the elongation at break of 227, 287, 242, 219, 229, 257%, respectively. The tensile strength of WPU1 is 1.54 times larger than that of WPU6. ISO is a rigid bicyclic structure which helps improve the mechanical properties of WPUs.[25] There are two main reasons for the result. Firstly, WPU1 samples had a higher degree of hydrogen bond interaction and micro-phase separation between the hard and hard segments.[32,33] Secondly, the hydrogen bonds interaction of N-H bond and ether oxygen were much stronger than carbonyl hydrogen bonds interaction.[34]

Thermal Degradation Properties Analysis. The effect of ISO on the thermal stability was analyzed by thermogravimetric analysis (TG). The results are shown in Figure 10, and the corresponding data are given in Table 5. Generally, the decomposition process of WPU is divided into several parts: the water of film was evaporated at 0-200 °C; followed by the

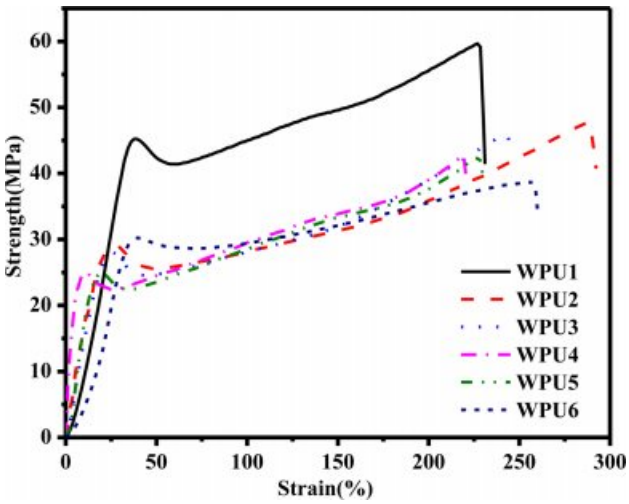

Figure 9. Stress-strain curves of WPU films.

breakdown of the hard segments (including the decomposition of the urea and carbamates), the decomposition temperature of the soft segments (polyethers or polyesters) at the end.[35,36] As shown in Figure 10(a), WPUs show almost no change at all in heat resistance with the content of ISO increased. However, as shown in Figure 10(b), $T_{d,urea,max}$ increased from 316 to 337 °C, $T_{d,urethane,max}$ rised from 373 to 392 °C, $T_{d,soft,max}$ increased from 452 to 472 °C with the content of ISO increased. The result might be attributed two reasons. Firstly, the rigidity of ISO limits the movement of the segment so that needs more energy to decomposition of all parts.[25] Secondly, the addition of ISO increased the order of internal structure of WPUs, the molecular chain was arranged regularly, and more energy dissociation was needed during the decomposition process.[37]

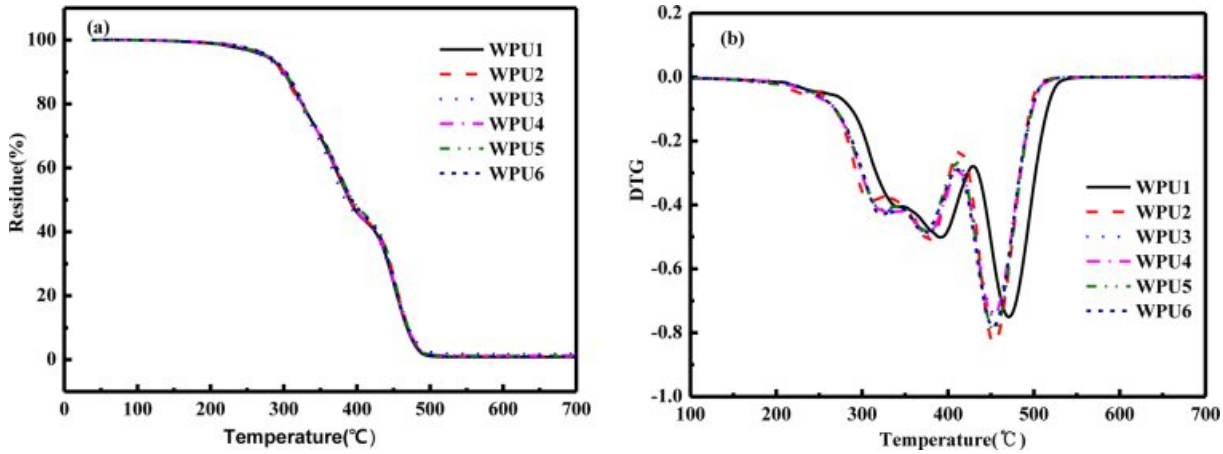

Figure 10. TGA curves of the WPU films: (a) TG curves; (b) DTG curves.

Table 7. Different WPU Films of Coating Performance

Samples	Contact angle (°)	W_{water} (%)	$W_{acetone}$ (%)	$W_{ethanol}$ (%)	W_{DMF} (%)	Pencil hardness	Adhesion
WPU1	70	6.06	52.08	305.00	498.36	2H	3B
WPU2	78	5.99	55.50	354.12	Partial Dissolved	3H	4B
WPU3	82.3	4.99	67.44	405.54	Dissolved	2H	4B
WPU4	83.4	3.81	77.59	Swelling	Dissolved	2H	4B
WPU5	84.95	3.17	78.46	Swelling	Dissolved	1H	5B
WPU6	85.6	3.06	90.91	Dissolved	Dissolved	1H	4B

Coating Performance Analysis. Nowadays, WPU was widely used as coatings to protect materials.[38] WPU had poor chemical resistance, adhesions and hardness compared with solvent polyurethane.[39] Thus these properties need to be further improved. ISO is a renewable resource with excellent mechanical properties. However, some researchers think ISO-based WPUs were still not available for coatings.[18] For this reason, the chemical resistance, pencil hardness and adhesion were characterized on WPU films in this work. Eventually, ISO was proved to improve some disadvantages on WPU coatings.

Table 7 shows coating performance of WPU films. The influence of ISO on the hydrophobicity was tested by static contact angle instrument on WPU films. With the content of ISO increased, the contact angle of WPU films was getting smaller. And the water resistance is getting worse, which is consistent with the result of the contact angle test. This may be attributed to the fact that ISO was hydrophilic.[18]

However, the WPU films are more excellent in resistant to acetone, ethanol and DMF. The rigid structure of ISO and ether oxygen group, and hard segments were more likely to aggregate into hydrogen bonds, as well as to form physical crosslinks. Hardness was increased when the WPUs system contain ISO, which might be attributed to ISO with the rigidity and ether oxygen group so that the system of hydrogen bonds formed the physical crosslinking network.[28]

With the content of ISO increased, the adhesion increased and then decreased. This may be ascribed to the fact that the ISO is a non-conjugated rigid structure which non-planar structure prevented closely packing between molecular chains.[25] However, ISO had a hydrophilic so that WPU films had better adhesion to the substrate when system had a proper the content of ISO. In summary, the proper content of isosorbide improves coating performance.

Conclusions

In this work, series of WPUs were successfully synthesized by using ISO as small molecule chain extender which was introduced to replace part of TMPD. The effects of ISO on the emulsion morphology and film properties of WPUs were stud-

ied. The molecular weight of WPUs was characterized by GPC. Meanwhile, the particle size distribution of WPU dispersions showed a single peak, peak firstly narrows and then unchanged. Moreover, the average particle size also firstly became larger and then unchanged. The result of FTIR showed that with the content of ISO increased, hydrogen bond interaction of the carbonyl group of WPUs decreased, and hydrogen bond interaction of the etheroxy group increased. The DSC and DMTA tests further demonstrated that ISO increased the hydrogen bond interaction in the WPUs. With the content of ISO increased, the degree of hydrogen bond interaction increased between the hard segment and the hard segment. The degree of micro-phase separation increased between the soft segment and the hard segments. Because of micro-phase separation and hydrogen bond interaction, the addition of ISO greatly increased the tensile strength of the WPU films. The result of XRD proved that ISO increased the degree of hydrogen bonding. The tensile strength of WPU1 was 59.67 MPa, which was 1.54 times higher than that of WPU6. The rigidity of ISO limits the movement of the segment so that needs more energy to decomposition of all parts. Therefore, the thermal gravimetric analysis of WPUs was also influenced when ISO was added. The addition of ISO increased the maximum degradation temperature of the hard segment and the soft segment of WPU films. The coating performance analysis showed that the addition of ISO improved the chemical resistance of the coating, and the pencil hardness of the coating also increased.

Acknowledgements: This study was supported by Natural Science Foundation of Anhui Province (1808085ME156) and University Natural Science Research Project of Anhui Province (KJ2018ZD004).

References

1. K. M. Zia, A. Noreen, M. Zuber, S. Tabasum, and M. Mujahid, *Int. J. Biol. Macromol*., **82**, 1028 (2016).
2. J. Y. Jung, J. M. Lee, S. K. Hong, J. K. Lee, H. M. Jung, and Y. S. Kim, *Polym. Korea*, **39**, 235 (2015).
3. T. Jiang, W. Wang, D. Yu, D. Huanf, N. Wei, Y. Hu, and H. Huang, *J. Polym. Res*., **25**, Article 140 (2018).
4. S. Oprea, V.-O. Potolinca, and V. Oprea, *Eur. Polym. J*., **83**, 161 (2016).
5. H. Blache, F. Méchin, A. Rousseau, E. Fleury, J.-P. Pascault, P. Alcouffe, N. Jacquel, and R. S.-Loup, *Ind. Crops Prod*., **121**, 303 (2018).
6. S. Lee, S. Kim, and I. K. Hong, *Polym. Korea*, **39**, 287 (2015).
7. R. Marín, A. Alla, A. M. de Ilarduya, and S. M.-Guerra, *J. Appl. Polym. Sci*., **123**, 986 (2012).
8. T. Calvo-Correas, M. D. Martin, A. Retegi, N. Gabilondo, M. A. Corcuera, and A. Eceiza, *ACS Sustainable Chem. Eng*., **4**, 5684 (2016).
9. I. Javni, O. Bilić, N. Bilić, Z. S. Petrovic, E. A. Eastwood, F. Zhang, and J. Ilavsky, *J. Appl. Polym. Sci*., **132**, 42830 (2015).
10. I. Javni, O. Bilić, N. Bilić, Z. S. Petrovic, E. A. Eastwood, F. Zhang, and J. Ilavsky, *Polym. Int*., **64**, 1607 (2015).
11. J. H. Han, H. J. Kim, and Y. T. Hong, *Polym. Korea*, **42**, 670 (2018).
12. X. Han, C. Tao, Z. Xie, J. Bao, Y. Huang, and G. Xu, *Polym. Korea*, **41**, 378 (2017).
13. Y. S. Ko and J. H. Yim, *Polym. Korea*, **37**, 587 (2013).
14. X. Yin, C. Dong, C. Chai, and Y. Luo, *Prog. Org. Coat*., **122**, 119 (2018).
15. C. Lee, E. Y. Jeong, and N. J. Jo, *Polym. Korea*, **42**, 320 (2018).
16. Y. Xia and R. C. Larock, *ChemSusChem*, **4**, 386 (2011).
17. Y. Li, B. A. J. Noordover, R. A. T. M. van Benthem, and C. E. Koning, *Eur. Polym. J*., **59**, 8 (2014).
18. Y. Li, B. A. J. Noordover, R. A. T. M. van Benthem, and C. E. Koning, *Eur. Polym. J*., **52**, 12 (2014).
19. C. Zhang, Z. Ren, Z. Yin, H. Qian, and D. Ma, *Polym. Bull*., **60**, 97 (2008).
20. H. S. Lee, Y. K. Wang, W. J. MacKnight, and S. L. Hsu, *Macromolecules*, **21**, 270 (1988).
21. Y. S. Kwak, E. Y. Kim, B. H. Yoo, and H. D. Kim, *J. Appl. Polym. Sci*., **94**, 1743 (2004).
22. E. Princi, S. Vicini, K. Castro, D. Capitani, N. Proietti, and L. Mannina, *Macromol. Chem. Phys*., **210**, 879 (2009).
23. M. Špírková, J. Pavličević, A. Strachota, R. Poreba, O. Bera, L. Kaprálková, J. Baldrian, M. Šlouf, N. Lazić, and J. Budinski-Simendić, *Eur. Polym. J*., **47**, 959 (2011).
24. L. Hong, L. Shi, and X. Tang, *Macromolecules*, **36**, 4989 (2003).
25. Y. Ma, J. Liu, M. Luo, J. Xing, J. Wu, H. Pan, C. Ruan, and Y. Luo, *RSC Adv*., **7**, 13886 (2017).
26. H. Pan and D. Chen, *Eur. Polym. J*., **43**, 3766 (2007).
27. L. Wang, Y. Shen, X. Lai, Z. Li, and M. Liu, *J. Polym. Res*., **18**, 469 (2011).
28. E. Kontou, G. Spathis, M. Niaounakis, and V. Kefalas, *Colloid Polym. Sci*., **268**, 636 (1990).
29. J. Łukaszczyk, B. Janicki, and M. Kaczmarek, *Eur. Polym. J*., **47**, 1601 (2011).
30. C. Fang, X. Zhou, Q. Yu, S. Liu, D. Guo, R. Yu, and J. Hu, *Prog. Org. Coat*., **77**, 61 (2014).
31. M. Durand, Y. Zhu, V. Molinier, T. Féron, and J.-M. Aubry, *J. Surfactants Deterg*., **12**, 371 (2009).
32. L. H. Bao, Y. J. Lan, and S. F. Zhang, *Iran. Polym. J*., **15**, 737 (2006).
33. W.-T. Lin and W.-J. Lee, *Colloids Surf. A: Physicochem. Eng.*

Asp., **522**, 453 (2017).
34. C. C. Santos, M. C. Delpech, and F. M. B. Coutinho, *J. Mater. Sci*., **44**, 1317 (2009).
35. Y. Du, J. Zhang, and C. Zhou, *Polym. Bull*., **73**, 293 (2016).
36. H. K. Shendi, I. Omrani, A. Ahmadi, A. Farhadian, N. Babanejad, and M. R. Nabid, *Prog. Org. Coat*., **105**, 303 (2017).
37. M. A. Corcuera, L. Rueda, B. F. d'Arlas, A. Arbelaiz, C. Marieta, I. Mondragon, and A. Eceiza, *Polym. Degrad. Stab*., **95**, 2175 (2010).
38. M. Akbarian, M. E. Olya, M. Ataeefard, and M. Mahdavian, *Prog. Org. Coat*., **75**, 344 (2012).
39. G. T. Howard, *Int. Biodeter. Biodegr*., **49**, 245 (2002).